Journal of Power Sources 250 (2014) 306–312

Contents lists available at ScienceDirect

Journal of Power Sources

journal homepage: www.elsevier.com/locate/jpowsour

Experimental investigation of axially non-uniform catalysis for methanol steam reforming

Guoqiang Wang [a,b], Feng Wang [a,*], Longjian Li [b], Guofu Zhang [b]

[a] Key Laboratory of Low-grade Energy Utilization Technologies and Systems, Chongqing University, Ministry of Education, Chongqing 400044, PR China
[b] College of Power Engineering, Chongqing University, Chongqing 400030, PR China

HIGHLIGHTS

- The performance of coating bed of uniform distribution is superior to packed bed.
- The catalyst activity distribution of coating-bed I turns out to be the optimal.
- The minimal temperature of 3 K has been detected in the case of coating bed I.
- The highest conversion of coating-bed I is 9.84% higher than the uniform case.

ARTICLE INFO

Article history:
Received 17 June 2013
Received in revised form
24 October 2013
Accepted 2 November 2013
Available online 15 November 2013

Keywords:
Non-uniform catalysis
Cold spot temperature
Temperature profile
Plate-type reactor
Methanol steam reforming

ABSTRACT

To enhance the hydrogen production, we designed a plate-type reactor to investigate the effect of the catalyst activity distribution on methanol steam reforming. The methanol steam reforming performance on a commercial $CuO/ZnO/Al_2O_3$ catalyst in a packed bed and a coating bed were compared experimentally. We found that higher conversion was achieved for the coating bed of uniform axial catalyst distribution compared to the packed bed. The cold spot temperature difference is restricted by using a higher fraction of inert particles at the inlet of the reactor and using a lower fraction of inert particles near the outlet of the reactor. Alleviating the cold spot difference can contribute to the improvement of the reactor performance. The minimum temperature of 3 K was determined in the case of coating bed I. This improvement results from the use of the appropriate non-uniform catalyst distribution to induce a favorable interaction among the mass and heat transfers. The highest conversion of 96.26% was achieved at the inlet weight hourly space velocity of 0.97 h^{-1} when the temperature was 543 K.

1. Introduction

Methanol can be converted to hydrogen at lower temperature than most other fuels because it contains no carbon–carbon bonds that must be broken. Methanol can be produced from a variety of sources, such as natural gas, coal, and biomass [1]. In industry, methanol is primarily formed from natural gas. The energy balance moving from syn-gas to methanol and then back to hydrogen is negative [2]. However, methanol is an excellent hydrogen carrier and a reasonable energy carrier, and it does not suffer from storage and transportation issues [3]. Compared with hydrogen, methanol provides easier and safer transportation [1]. This conversion of methanol to hydrogen is justified because the reformation of liquid fuels may become an important process for hydrogen production for on-site stationary fuel cell or on-board mobile fuel cell applications [4]. From a health viewpoint, methanol is worse than some fuels but better than others. For example, methanol is safer than gasoline but is less safe than diesel. Methanol ingestion is the primary health concern because it produces formic acid in the human body when metabolized [5]. The overall absorption rate of methanol was found to be much less than its metabolism rate, even in a worst-case exposure situation [6]. Fuels for hydrogen production are numerous, and decisions on the choice of fuel are made based on which parameter is deemed most important for the system. Because methanol is inherently a synthetic fuel, it does not suffer from sulfur contamination [7,8]. Because a system does not require a front-end desulphurization operation or sulfur-tolerant catalysts to operate on methanol, methanol is very favorable for hydrocarbon reforming [9]. The methanol steam reforming approach could obtain lower CO production in the products compared to other methanol conversion methods. As a result, methanol steam reforming (MSR) is generally the most economic approach to

* Corresponding author. Tel.: +86 013618203569.
E-mail address: wangfeng@cqu.edu.cn (F. Wang).

0378-7753/$ – see front matter © 2013 Elsevier B.V. All rights reserved.
http://dx.doi.org/10.1016/j.jpowsour.2013.11.007

producing H_2 [2]. The catalytic production of hydrogen by methanol steam reforming is an attractive option for on-site stationary fuel cell or onboard mobile fuel cell applications [3]. The conventional packed bed MSR method, which is widely used in industry, suffers from axial temperature gradients and the problems such as the occurrence of cold spots [8]. These disadvantages result from the severe limitations of mass and heat transfer [10]. These axial temperature gradients lead to thermal stresses in the channels [11]. Catalyst performance characteristics, such as stability and durability, are significantly affected by the thermal stresses [12]. Furthermore, because of the severe transfer resistance, conventional steam reformers are limited to an effectiveness factor of the catalyst that is typically less than 5% [13].

The $CuO/ZnO/Al_2O_3$ catalyst has been extensively used in methanol reforming [14]. It is generally agreed that the active component in the $CuO/ZnO/Al_2O_3$ catalyst is copper [15]. The role of ZnO is regarded as relatively minimal, but it is required as a textural support in segregating the Cu, which is highly susceptible to sintering [16]. The use of alumina creates a high surface area support that serves to increase copper dispersion and decrease the susceptibility to sintering [17]. Maintaining an optimum oxidization state is an important feature of the commercial $CuO/ZnO/Al_2O_3$ catalyst [14]. Research groups have sought to develop a novel catalyst to achieve improved performance in methanol reforming. Takahashi reported that an amorphous CuZrPd alloy catalyst was formed by adding palladium to a CuZr catalyst. Although the CuZrPd alloy accelerated methanol conversion, it produced more CO than CuZr alone because this alloy facilitated methanol decomposition [18,19]. Karim and Dagle reported that Pd was eventually alloyed with Zn and PdZn crystallites, resulting in the production of more CO [20,21]. Velu et al. studied methanol steam reforming over CuZnAl(Zr)-oxide catalysts. The surface area and dispersion of Cu were found to be improved by adding Zr to the CuZnAl catalyst. However, CO_2 and CO were both found to be primary products [22,23]. Precious metals and other group VIII metals exhibit more active performance for methanol conversion [24]. However, they predominantly catalyze methanol decomposition and are not selective for the methanol reforming reaction [25]. Although noble metal catalysts dealt with the problem of the sintering and deactivation of Cu-based catalysts at high temperature, the high cost and the production of more CO remain problematic because it is acknowledged that CO is a poison for the anode electro catalyst of proton exchange membrane fuel cell [18]. In addition, the catalyst accounts for a high portion of the reactor operating cost. As a result, we used the commercial $CuO/ZnO/Al_2O_3$ catalyst for our study.

Micro-reactors are also used because their high surface-to-volume ratio and short conduction paths are able to offer a higher heat transfer rate than the traditional chemical reactors [26]. The small diameters of the reactor channels ensure a short radial diffusion time, leading to a high heat transfer coefficient, which is advantageous because the heat transfer coefficient is known to influence the homogeneously catalyzed reaction [27]. Thus, micro-reactors are increasingly recognized in recent years as a novel tool for chemistry and chemical process. Deqing Mei and Wei Zhou enhanced the performance of hydrogen production through the use of a micro-reactor [28,29]. B. H Howard achieved a 90% conversion efficiency by integrating a micro-channel heat exchanger [30]. However, several difficulties and challenges persist. Ayman Karim investigated the effect of reactor diameter on the cold spot temperature difference, and he found that the MSR in a packed bed reactor only 1 mm in diameter suffered from a cold spot temperature difference of up to 22 K due to the heat transfer limitation [31,32]. Moreover, the temperature difference or cold spot could be removed only when the equivalent diameter was as small as 300 μm [31]. Unfortunately, such micro-scale reactors are impractical for real industrial applications. One problem is that the characteristics of such micro-scale reactors lead to a large amount of heat losses from the reactor to the ambient because micro-reactors exhibit high specific surfaces [26]. Another problem is the difficulty in introducing the catalytic active phase into the micro-channel when using micro-reactors in heterogeneously catalyzed gas-phase reactions [33]. In addition, each channel must be packed identically to avoid misdistribution because random packing would result in a high-pressure drop [33].

The reforming reactions are a complex catalytic process consisting of multicomponent flow and diffusion. A reforming reaction is controlled not only by the kinetics of the reaction but also by the catalyst activity and thermal effects load at local position [1]. Dalla Betta described a method to avert the hot spot problem, which is a factor for coking and unsatisfactory reactor yield, by using a graded catalyst distribution in a highly exothermic methanol combustion reaction [34,35]. Tronci demonstrated that non-uniform distributions could shift the light-off position towards the inlet of the monolith [12]. Quina and Berger applied catalyst dilution to produce a higher yield without increasing the peak temperature [36]. Sung-won Hwang used side-streams and inert pellets to control the temperature profiles; the feed-stream distribution could not reduce temperature peak as effectively as catalyst dilution [29,37]. This behavior is attributed to the superior thermal management in local areas.

This study aims to investigate the effect of the catalyst activity distribution on methanol steam reforming and to compare the performance of a packed bed to a coating bed. The use of catalyst dilution was explored to reduce the reaction rate and heat consumption at critical points inside the plate-type reactor. While the total catalyst amount was kept constant, the dilution ratios in the three different coat-beds were used to control the temperature profile at the maximization of yield. Because the degree of stream bypass depends on the degree of segregation of the catalyst and the diluents, the catalyst is sufficiently well mixed with the inert particles to prevent the conversion decrease.

2. Experimental apparatus

2.1. Plate-type reactor design

Two chambers were integrated into a plate-type stainless steel micro-reactor. The steam of water and methanol was superheated before entering the 6 mm × 6 mm × 125 mm reaction chamber. Holes 1.5 mm in diameter, for measuring the temperature, were arranged axially in the cover plate of the reaction chamber. The axial temperatures of the reaction chamber were monitored using T-type thermocouples, as shown in Fig. 1.

2.2. Packed bed design and preparation

The commercial $CuO/ZnO/Al_2O_3$ catalyst (CB-7) from Chuanhua Co. Ltd. was used in all the experiments. For the packed bed, the catalyst was crushed and sieved to a particle size of approximately 0.5 mm. Next, 3.5 g of the catalyst was homogeneously mixed with 1.6 g of quartz particles (0.5 mm in diameter), which exhibited no catalysis for this reaction, and then, the mixture was uniformly packed into the reaction chamber.

2.3. Coating bed design and preparation

Slabs of commercial aluminum were used as supports. The dimensions of the support samples were 20 mm × 6 mm and 1 mm in height. The supports were pre-treated before wash coating. The

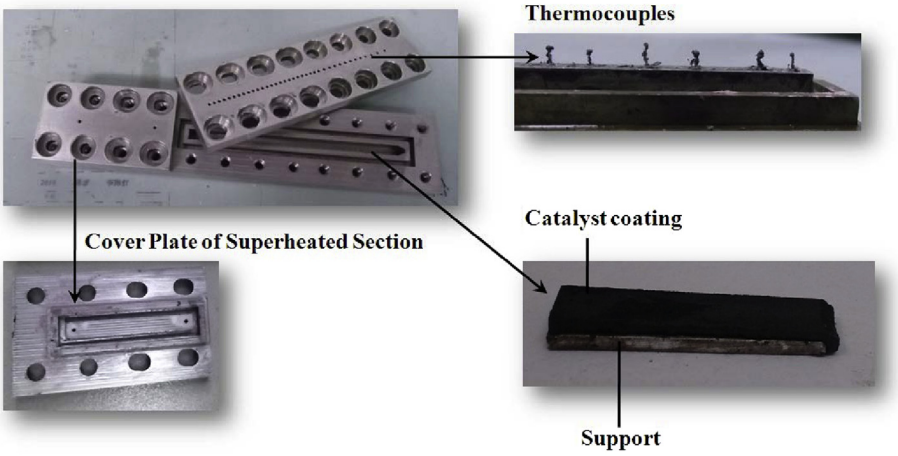

Fig. 1. Images of the reactor and coating-bed.

supports were immersed in HCl solutions at room temperature to improve the surface roughness, and they were subsequently immersed in HNO_3 solutions at 80 °C to favor the formation of surface oxides. The surfaces were rinsed with DI H_2O and dried in an oven. This support pre-treatment led to the formation of an alumina oxide layer, which greatly improved the adherence of the deposited γ-Al_2O_3 layers [38,39].

The gels were prepared by dispersing boehmite, which was used as a binder and did not catalyze the reaction, with hydrochloric acid. First, the water and boehmite were initially combined in the mass ratio of 1:16 (boehmite/DI-water). After vigorous stirring for approximately 4 h, the boehmite/DI-water was quickly raised to the temperature of 85 °C. Next, hydrochloric acid was slowly added to disperse the flocculated boehmite powder to create a colloidal suspension. The CuO/ZnO/Al_2O_3 catalyst (less than 25 μm in diameter) was added to the gels, and the catalytic slurries were dispersed overnight. The ratio of catalyst to boehmite was controlled to change the level of the catalyst activity of the catalytic coatings. For the previous coating procedure, the support was withdrawn from the slurries and dried at room temperature for 1 h. A stainless steel mold was used to deposit the slurries after the above coating procedure was repeated 3 times. For a later coating procedure, the support coated with the catalytic slurries was loaded into the mold placed on an electric heating plate. The slurries were added into the mold step by step, dried at 80 °C, and then extruded under the pressure of the mold. The later coating procedure was repeated until the coating reached the required weight. The Catalytic Panels containing different masses of catalyst were finally obtained on the support, as listed in Table 1. Coating-bed I was formed by packing the Catalytic Panels into the reaction chamber in the order of #1, #2, #3, #4, #5, while distribution III was formed by packing the mixture into the reaction chamber in the order of #5, #4, #3, #2, #1. A continuous arrangement of 5 #3 Catalytic Panels formed coating-bed II. As a result, each bed zone used a different portion of inert dilution to generate different activities, as shown in Fig. 2.

Table 1
Catalyst mass of Catalytic Panels.

Catalytic Panel	#1	#2	#3	#4	#5
Catalyst/boehmite (w/w)	3:7	9:11	3:2	3:1	9:1
Mass of catalyst (g)	0.12	0.18	0.24	0.30	0.36

2.4. Experimental procedures and analysis

The water/methanol (purity ≥99.5%) mixture with a molar ratio of 1.3:1 was used in all experiments. The experiments were performed after the catalyst reduction. All experiments were performed under atmospheric pressure. The reactor effluent stream was cooled and condensed by the condenser, and an ice trap before a soap foam flow meter was used to measure the total dry product gas. A gas chromatograph (GC-3000) equipped with a Porapak Q column and a TCD detector, with helium as the carrier gas, was used to analyze the effluent. The mole fraction of each component was obtained by performing a material balance calculation [40].

3. Results and discussions

3.1. MSR on packed bed

The three main reactions for this combination of reactants and products can be described by the following three equations [41].

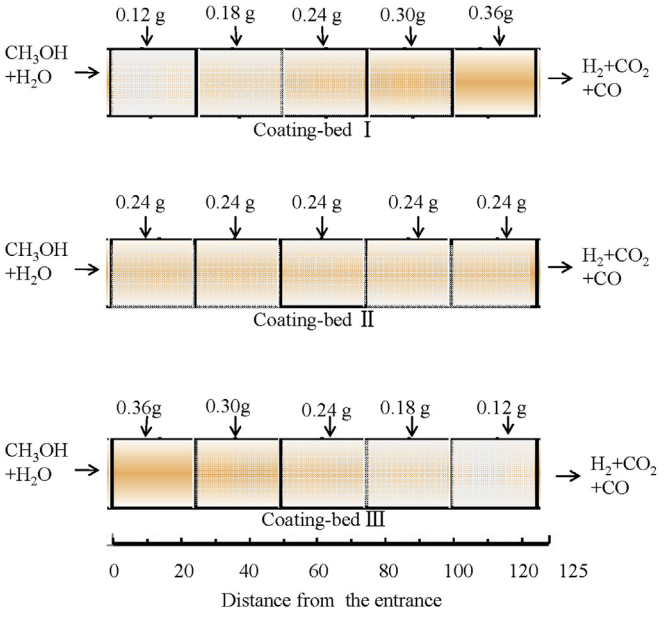

Fig. 2. Catalyst distribution of coating-beds.

$$CH_3OH + H_2O \rightarrow 3H_2 + CO_2 \quad \Delta H^o_{298} = +49.4 \text{ KJ mol}^{-1} \quad (1)$$

$$CH_3OH \rightarrow CO + 2H_2 \quad \Delta H^o_{298} = +92.0 \text{ KJ mol}^{-1} \quad (2)$$

$$CO + H_2O \leftrightarrow CO_2 + H_2 \quad \Delta H^o_{298} = -41.1 \text{ KJ mol}^{-1} \quad (3)$$

Eq. (2) represents the methanol decomposition and Eq. (3) represents the water gas shift reaction. Eq. (1) is the algebraic summation of Eqs. (2) and (3). The major products of H_2 and CO_2, together with a small quantity of CO, were detected in the reformate. Fig. 3 shows the methanol conversion and hydrogen production rate under the different WHSV (weight hourly space velocity). A high WHSV causes the resident time of the reactant to be decreased, causing the reforming reaction to not be completed in the catalyst bed. As a result, the methanol conversion and hydrogen production rate is decreased with an increasing WHSV under the same reaction temperature. In addition, the hydrogen production rate is increased within a certain range of WHSV. Fig. 3 also shows that the methanol conversion and hydrogen production rate are favored by high temperature. Because MSR is highly endothermic, a high temperature suppresses reaction (3) and favors reactions (1) and (2). As a result, more methanol can be converted into H_2. This result agrees with the results of references [42].

When the inlet temperature of the catalyst bed is 543 K, the temperature profile is obtained as shown in Fig. 4. The temperature along the reactor is not constant at 543 K; rather, it is initially

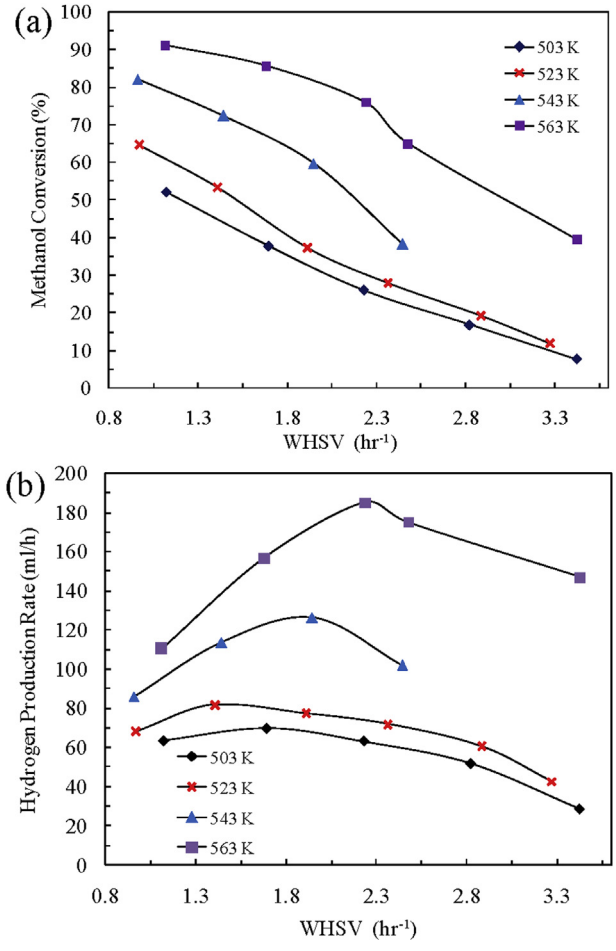

Fig. 3. (a) Methanol conversion and (b) hydrogen production rate for the packed-bed with different temperature under the different WHSV.

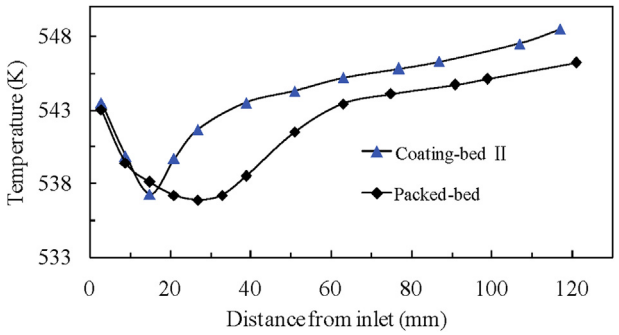

Fig. 4. Temperature profiles along bed length.

depressed, then elevated. At the position 22 mm away from the inlet, a cold spot temperature difference of 6 K is detected. This temperature difference could be explained by the limitations of both heat and mass transfer. During the methanol steam reforming, the reactants diffuse into the porous structure and react on the active sites. The products subsequently diffuse through the pores back into the bulk. As the reaction proceeds in the catalyst layer, energy is released and transferred to the solid and gas phases by conduction and convection. A key problem is the balance between the heat supply through the reformer and the heat consumption in the endothermic reforming reaction. This heat balance makes heat transfer a significant factor. However, the conduction through the tube wall to the catalyst pellets is limited by the high thermal contact resistance and the low thermal conductivity of the catalyst pellets. Additionally, the convection is weakened because of the low flow velocity of the mixture in the catalyst bed. Thus, for a packed bed with a uniform catalyst distribution, the rate of heat supply is lower than that of heat consumption due to the limitation of heat transfer. Furthermore, the reactant diffusion rate may be lower than the reactant chemical reaction rate, which would lead to a limitation of mass transfer. A dominant amount of reactant molecules could be converted to the reformate before they diffuse to the surface of the catalyst, which is located near the outlet. Therefore, the reactant concentration has a maximum value at the inlet of the catalyst bed, while it will progressively decrease along the axis of the reactor due to the mass transfer limitation. Because a high reactant concentration could accelerate the reaction, the heat required by the reaction could reach a peak at the inlet of the reaction chamber, where the “cold spot” occurs. Thus, due to the low axial and radial heat conductivity, an axial temperature gradient develops in conventional reactors with randomly packed beds. Such a temperature gradient can lead to stresses in the substrate, catalyst deactivation and subsequent degradation [43–45]. This cold spot temperature difference makes the MSR perform at a temperature lower than the optimal catalyst operation temperature because it reduces the catalyst activity.

3.2. Comparison of a packed bed and a coating-bed for MSR

MSR is a heterogeneous catalytic reaction whose reaction rate is affected by diffusion limitations, the reactant concentration and the catalyst surface temperature. The temperature of local sites in the beds is an important factor, which affects the performance of the reformer. For coating bed II, we compared a packed bed to a coating bed. The temperature profiles along the bed length in the two catalyst beds are shown in Fig. 4. The outlet temperature and the average temperature are higher in coating bed II than in packed bed II. In coating bed II, the methanol conversion and hydrogen production rate are superior to the packed bed case, as shown in Fig. 5. The contributing factor is that the heat transfer is improved due to

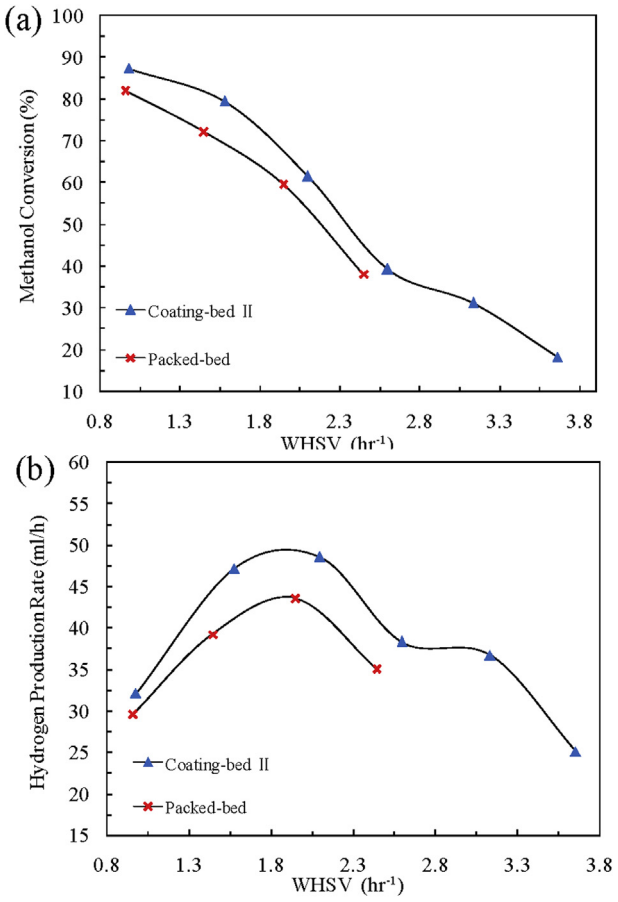

Fig. 5. (a) Methanol conversion and (b) hydrogen production rate comparing for packed-bed and coating-bed II.

the lower thermal contact resistance compared to the packed bed. Thus, the temperatures in the coating bed are higher than in the packed bed. Although the scope of influence of the cold spot was reduced, the cold spot differences in the two cases appeared to be equal.

3.3. *Effect of catalyst distribution on the catalytic reaction*

Transfer limitations in strong endothermic methanol steam reforming can lead to axial temperature gradients, which cause thermal stresses in the channels. Because catalyst lifetime is limited by thermal stresses, the catalyst performance can be improved by alleviating the axial temperature gradients. To investigate the effect of catalyst activity distribution on methanol steam reforming, three types of activity distributions were designed at a given catalyst amount. According to the distribution results, the active materials in coating bed I are at a minimum concentration near the entrance, with the concentration increasing along the bed length. In coating bed II, the concentration of active materials remains constant axially. The active materials in coating bed III are at a maximum concentration near entrance, with the level decreasing axially. The redistribution of the active component concentration and reactant concentration can result in variations in the outlet reactant conversion. Fig. 6 shows the axial temperature profiles of four beds at an inlet temperature of 543 K. The minimal cold spot difference of 3 K was observed for coating bed I, with the difference increasing to the maximum of 8 K for coating bed III. At an inlet temperature of 543 K, the methanol conversion and hydrogen production rate are plotted as a function of temperature in Fig. 7. Using coating bed I, a

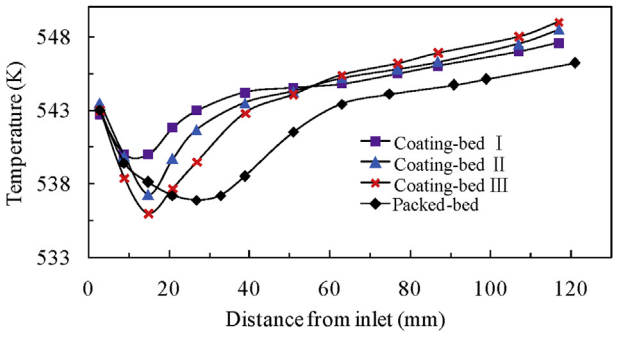

Fig. 6. Axial temperature distributions in four catalyst beds.

significant improvement in the reactor performance was observed. The use of coating bed I, with a minimal cold spot temperature difference, produced a higher methanol conversion and a higher hydrogen production rate than the other two coating beds. The use of coating bed III for methanol conversion resulted in the decrease of the methanol conversion and hydrogen production rates compared to the rates when the packed bed was used. Fig. 7(a) shows that a methanol conversion of 96.26% was achieved when the value of WHSV was 0.97 h^{-1} in coating bed I. However, using coating bed III, the conversion drops to 74.9% at a WHSV of 0.98 h^{-1}. At approximately a WHSV of 1.91 h^{-1}, the hydrogen production rate drops from 58.39 ml min^{-1}–39.88 ml min^{-1} when the case is

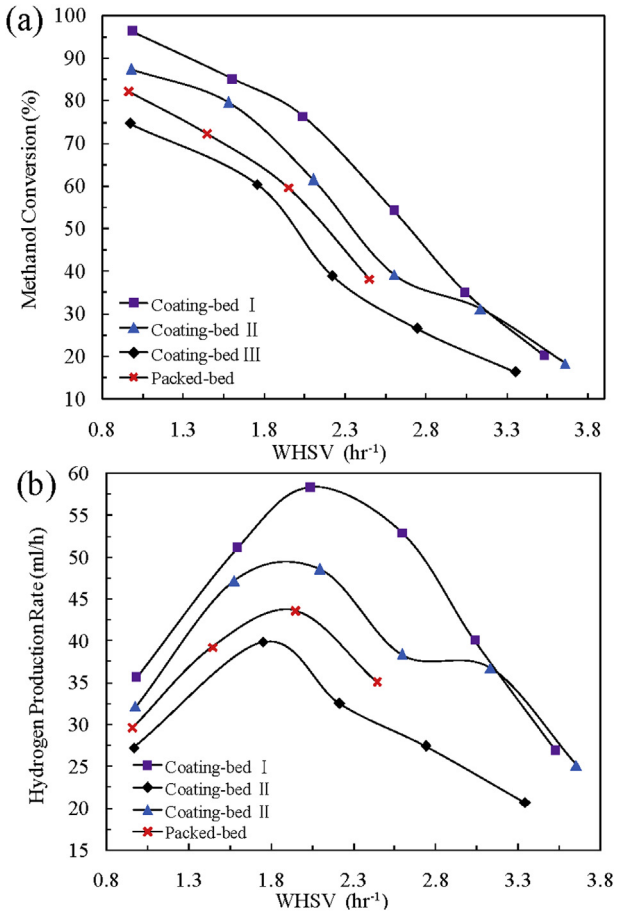

Fig. 7. (a) Methanol conversion and (b) Hydrogen production rate as function of WHSV.

moved from coating bed I to coating bed III, as shown in Fig. 7(b). The underlying reason for this improvement is that the appropriate non-uniform catalyst distribution can induce a favorable interaction between the mass transfer and heat transfer. In addition, the local thermal management was intensified. In coating bed I, a lower amount of catalyst was situated near the inlet. The reaction was weakened due to the diminishing amount of the catalyst at the reactor inlet. This reduced amount of catalyst leads to a decrease in the heat absorption by the reaction in the local areas. Thus, the cold spot temperature difference can be reduced by adjusting the amount of catalyst in local areas. A higher amount of catalyst could be used when the isothermal condition of the working temperature is reached. Therefore, the catalytic reforming performance is improved due to the improvement of the catalyst utilization. Conversely, in coating bed III, the catalytic reaction was strengthened because more catalyst is used, but the enlarged cold spot temperature difference leads to a decrease in the efficiency of the catalyst utilization. Many new highly active catalysts contain precious metals, which noticeably increases the catalyst cost in the overall cost of the process. Optimization of the active component distribution is a method of cost savings because the hydrogen yield increased at a given catalyst load.

Fig. 8 shows the methanol conversion and hydrogen production rate at different temperatures. The highest conversion and hydrogen production rate was achieved using coating bed I. Furthermore, more methanol can be converted to H_2 at a higher temperature. Although a higher temperature has a positive influence on the reaction conversion, it leads to many problems. First, a slight increase in the maximum temperature may result in catalyst failure. Moreover, at a high temperature, more CO, which is poisonous to the fuel cell, is produced, while reaction (3) is favored. A high temperature would result in carbon formation, which is the primary cause of catalyst deactivation and is deleterious for methanol steam reforming. The CO concentration is plotted as a function of WHSV in Fig. 9. More CO was found to be generated at higher temperatures. Because more water leads to increased consumption of CO by the water gas shift reaction, the CO concentration is decreased with the increase of WHSV. Thus, methanol conversion and CO concentration should both be taken into consideration to achieve the desired temperature level for the reforming reaction in actual hydrogen production. In this work, the optimal temperature is 543 K when methanol conversion and CO concentration are both taken into consideration. The highest conversion efficiency of 96.26% was achieved at an inlet WHSV of 0.97 h^{-1} when the temperature was 543 K. This efficiency is 9.84% higher than that of coating bed II with a uniform distribution of catalyst. The highest hydrogen production rate is 58.39 ml min^{-1} at the conversion efficiency of 76.35% for a temperature of 543 K and a WHSV of 2.04 h^{-1}.

MSR was performed using coating bed I to evaluate the stability, which is a key factor for catalyst performance. During this test, the H_2 concentration and CO concentration were kept constant at 72% and 0.65%, respectively, as seen in Fig. 10. The methanol conversion exhibited a negligible decrease during the test. No noticeable catalyst deactivation was observed. As a result, coating bed I using the $CuO/ZnO/Al_2O_3$ catalyst represents a good and stable system for MSR.

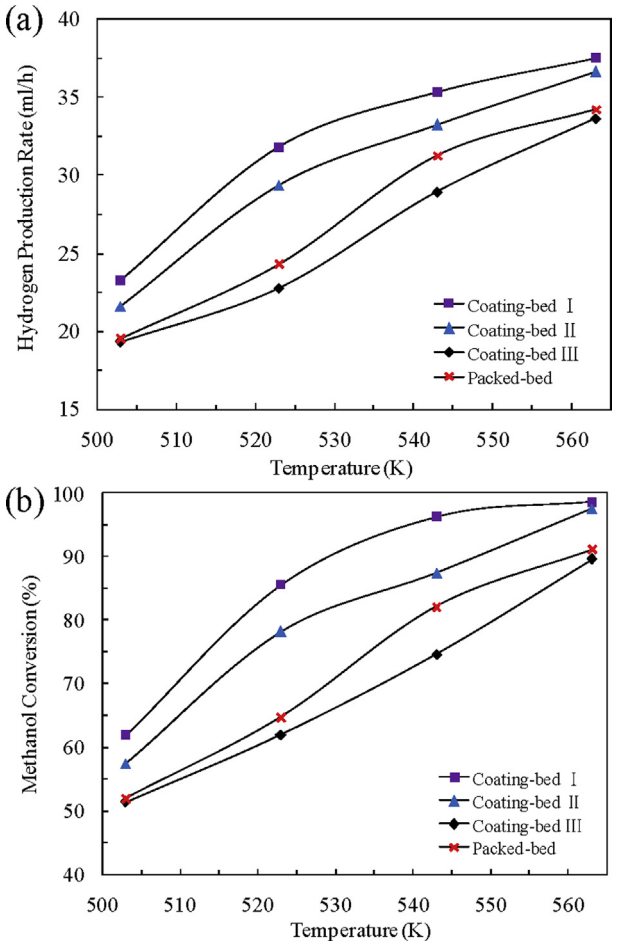

Fig. 8. (a) Methanol conversion and (b) Hydrogen production rate variations with temperature.

4. Conclusion

Catalytic Panels containing different amounts of active materials were fabricated by varying the catalyst dilution ratios. Three coating beds were produced by varying the order of the Catalytic Panels in a reaction chamber. MSR was performed using three different coating beds in a plate-type reactor. The results of the study on the effect of an axially non-uniform catalyst distribution on the temperature distribution and the outlet reactant conversion for MSR were presented. The results were compared to those of a packed bed. The use of a coating-bed of uniform distribution was found to be superior the use of a packed bed. Additionally, the non-uniform axial catalyst distribution of coating bed I was

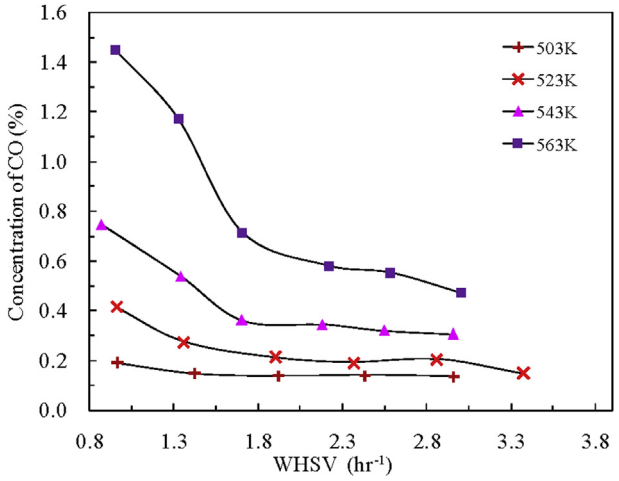

Fig. 9. CO concentration as a function of WHSV on coating-bed III.

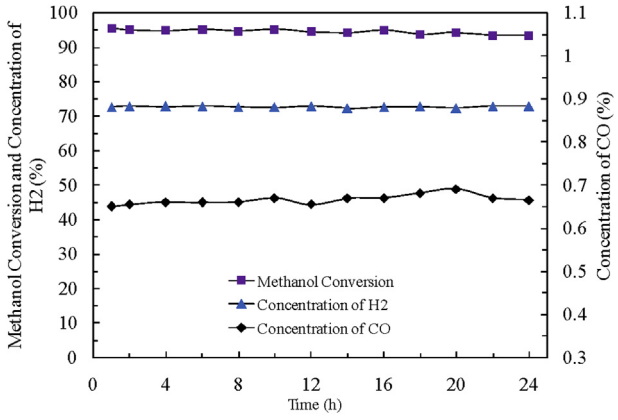

Fig. 10. Stability of coating-bed III with $CuO/ZnO/Al_2O_3$ catalyst.

demonstrated to offer better performance than the uniform distribution case. In coating bed I, a lower amount of catalyst is situated near the entrance, and more catalyst is situated at the outlet. For all the cases, the cold spot temperature difference was observed in temperature profiles. Alleviating the cold spot difference can improve the reactor performance. The underlying reason for this improvement is that the appropriate non-uniform catalyst distribution can induce a favorable interaction among the mass and heat transfer and the reaction. The minimal temperature difference of 3 K was observed in the case of coating bed I. When the temperature is 543 K, the highest conversion efficiency observed is 96.26%, which is 9.84% higher than that of the uniform case, and the largest hydrogen production rate is 58.39 ml min^{-1} at the conversion efficiency of 76.35%.

Acknowledgments

The authors acknowledge the support of National Natural Science Foundation of China (50906104).

References

[1] W.H. Cheng, S. Akhter, H.H. Kung, J. Catal. 82 (1983) 341–350.
[2] K. Subramanyan, U.M. Diwekar, J. Power Sources 142 (2005) 103–116.
[3] A. Szizybalski, F. Girgsdies, A. Rabis, Y. Wang, M. Niederberger, T. Ressler, J. Catal. 233 (2005) 297–307.
[4] J.D. Holladay, J.S. Wainright, E.O. Jones, S.R. Gano, J. Power Sources 130 (2004) 111–118.
[5] D.R. Palo, J.D. Holladay, R.T. Rozmiarek, C.E. Guzman-Leong, Y. Wang, J. Hu, Y. Chin, R.A. Dagle, E.G. Baker, J. Power Sources 108 (2002) 28–34.
[6] A.G. Dixon, D.L. Cresswell, AIChE J. 25 (1979) 663–676.
[7] A. Basile, S. Tosti, G. Capannelli, G. Vitulli, A. Iulianelli, F. Gallucci, E. Drioli, Catal. Today 118 (2006) 237–245.
[8] A. Basile, G.F. Tereschenko, N.V. Orekhova, M.M. Ermilova, F. Gallucci, A. Iulianelli, Int. J. Hydrogen Energy 31 (2006) 1615–1622.
[9] D.R. Palo, R.A. Dagle, J.D. Holladay, Chem. Rev. 107 (2007) 3992–4021.
[10] T. Kitahara, H. Nakajima, K. Mori, M. Inamoto, ECS Trans. 50 (2013) 437–444.
[11] T.J. Mason, J. Millichamp, T.P. Neville, P.R. Shearing, S. Simons, D.J. Brett, J. Power Sources 242 (2013) 70–77.
[12] S. Tronci, R. Baratti, A. Gavriilidis, Chem. Eng. Commun. 173 (1999) 53–77.
[13] S. Roy, B.B. Pruden, A.M. Adris, J.R. Grace, C.J. Lim, Chem. Eng. Sci. 54 (1999) 2095–2102.
[14] C.T. Vo, L.K. Huynh, J.Y. Hung, J. Jiang, Appl. Surf. Sci. 280 (2013) 219–224.
[15] B. Lindström, L.J. Pettersson, Int. J. Hydrogen Energy 26 (2001) 923–933.
[16] M.K. Agarwal, K. Nagi Reddy, H.B. Patel, J. Cryst. Growth 46 (1979) 139–142.
[17] J.L. Pinilla, R. Moliner, I. Suelves, M.J. Lázaro, Y. Echegoyen, J.M. Palacios, Int. J. Hydrogen Energy 32 (2007) 4821–4829.
[18] T. Kobayashi, J. Otomo, C. Wen, H. Takahashi, J. Power Sources 124 (2003) 34–39.
[19] T. Suda, T. Takahashi, P. Golstein, S. Nagata, Cell 75 (1993) 1169–1178.
[20] T. Conant, A. Karim, S. Rogers, S. Samms, G. Randolph, A. Datye, Chem. Eng. Sci. 61 (2006) 5678–5685.
[21] Y. Chin, R. Dagle, J. Hu, A.C. Dohnalkova, Y. Wang, Catal. Today 77 (2002) 79–88.
[22] S. Velu, K. Suzuki, M. Okazaki, M.P. Kapoor, T. Osaki, F. Ohashi, J. Catal. 194 (2000) 373–384.
[23] S. Velu, K. Suzuki, M.P. Kapoor, F. Ohashi, T. Osaki, Appl. Catal. A Gen. 213 (2001) 47–63.
[24] G. Jacobs, T.K. Das, Y. Zhang, J. Li, G. Racoillet, B.H. Davis, Appl. Catal. A Gen. 233 (2002) 263–281.
[25] S. Kameoka, T. Tanabe, A.P. Tsai, Catal. Lett. 100 (2005) 89–93.
[26] Y. Choi, H.G. Stenger, J. Power Sources 129 (2004) 246–254.
[27] G. Kolb, J. Schürer, D. Tiemann, M. Wichert, R. Zapf, V. Hessel, H. Löwe, J. Power Sources 171 (2007) 198–204.
[28] D. Mei, M. Qian, B. Liu, B. Jin, Z. Yao, Z. Chen, J. Power Sources 205 (2012) 367–376.
[29] D.J. Klionsky, F.C. Abdalla, H. Abeliovich, R.T. Abraham, A. Acevedo-Arozena, K. Adeli, L. Agholme, M. Agnello, P. Agostinis, J.A. Aguirre-Ghiso, Autophagy 8 (2012) 445–544.
[30] B.H. Howard, R.P. Killmeyer, K.S. Rothenberger, A.V. Cugini, B.D. Morreale, R.M. Enick, F. Bustamante, J. Membr. Sci. 241 (2004) 207–218.
[31] A. Karim, J. Bravo, D. Gorm, T. Conant, A. Datye, Catal. Today 110 (2005) 86–91.
[32] A. Karim, J. Bravo, A. Datye, Appl. Catal. A Gen. 282 (2005) 101–109.
[33] D. Gervasio, S. Tasic, F. Zenhausern, J. Power Sources 149 (2005) 15–21.
[34] M.B. Cutrone, K.W. Beebe, R.A. Dalla Betta, J.C. Schlatter, S.G. Nickolas, T. Tsuchiya, Catal. Today 47 (1999) 391–398.
[35] R.A. Dalla Betta, T. Rostrup-Nielsen, Catal. Today 47 (1999) 369–375.
[36] J. Pérez-Ramírez, R.J. Berger, G. Mul, F. Kapteijn, J.A. Moulijn, Catal. Today 60 (2000) 93–109.
[37] S. Hwang, C.M. Ballantyne, A.R. Sharrett, L.C. Smith, C.E. Davis, A.M. Gotto, E. Boerwinkle, Circulation 96 (1997) 4219–4225.
[38] M. Valentini, G. Groppi, C. Cristiani, M. Levi, E. Tronconi, P. Forzatti, Catal. Today 69 (2001) 307–314.
[39] S. Kikuchi, K. Satoh, T. Nagata, N. Kawagashira, K. Doi, N. Kishimoto, J. Yazaki, M. Ishikawa, H. Yamada, H. Ooka, Science 301 (2003) 376–379.
[40] D. Wu, H. Wang, B. Zhu, Z.Z., Y. Zhong, J. East China Univ. Sci. Technol. (in Chinese) 29 (2003) 120–123.
[41] G. Park, D.J. Seo, S. Park, Y. Yoon, C. Kim, W. Yoon, Chem. Eng. J. 101 (2004) 87–92.
[42] N. Viriya-Empikul, P. Krasae, B. Puttasawat, B. Yoosuk, N. Chollacoop, K. Faungnawakij, Bioresour. Technol. 101 (2010) 3765–3767.
[43] J.J. Thiart, S.M. Bradshaw, H.J. Viljoen, V. Hlavacek, Chem. Eng. Sci. 48 (1993) 1925–1932.
[44] S.T. Kolaczkowski, P. Plucinski, F.J. Beltran, F.J. Rivas, D.B. McLurgh, Chem. Eng. J. 73 (1999) 143–160.
[45] H.J. Viljoen, N. Van Rensburg, AIChE J. 41 (1995) 1341–1345.